

Characterization of Passive CMOS Strip Detectors After Proton Irradiation

Marta Baselga^{a,*}, Jan-Hendrik Arling^b, Naomi Davis^b, Jochen Dingfelder^c, Ingrid Maria Gregor^{b,c}, Marc Hauser^d, Fabian Hügging^c, Karl Jakobs^d, Michael Karagounis^e, Roland Koppenhöfer^d, Kevin Alexander Kröniger^a, Fabian Lex^d, Ulrich Parzefall^d, Simon Spannagel^b, Dennis Sperlich^d, Jens Weingarten^a, Iveta Zatocilova^d

^aFaculty of Physics, TU Dortmund, Otto-Hahn-Strasse 4a, 44227 Dortmund, Germany

^bDeutsches Elektronen Synchrotron DESY, Notkestr. 85, Hamburg, Germany

^cPhysikalisches Institut, University of Bonn, Nussallee 12, 53115 Bonn, Germany

^dPhysikalisches Institut, Albert-Ludwigs-Universität Freiburg, Hermann-Herder-Straße 3, Freiburg, Germany

^eFachhochschule Dortmund, Sonnenstraße 96, 44139 Dortmund, Germany

Abstract

Strip detectors are populating outer trackers of high-energy particle experiments. They are convenient for covering large areas of sensitive material since they use less power and have fewer readout channels compared to pixels sensors. Nevertheless, they are typically manufactured with a mask set that covers the full wafer, otherwise when using smaller reticles the strip implants have to be stitched. For this project, strip detectors were fabricated in a CMOS commercial foundry using different reticles to be stitched several times, proving the feasibility of this technology.

LFoundry produced the passive CMOS strip detector with a production line of 150 nm node technology, using a 150 μm thick FZ wafer. Those strip sensors have three different geometries to study different impacts of the CMOS technology. The strips have lengths of 2.1 cm and 4.1 cm, stitching 3 or 5 reticles respectively. This work shows results of 24 GeV proton irradiated passive CMOS strip detectors. The detectors were irradiated at CERN and were tested with different set-ups, not showing any effect from the strips stitching.

Proving that this technology is feasible for detecting high-energy particles opens the door to future large productions of passive strip detectors and also to produce active strip sensors in commercial CMOS foundries.

Keywords: Passive CMOS, silicon strip sensors, stitching, irradiation studies

1. Introduction

Future experiments tracking systems for high-energy particle detection will most probably be populated with silicon sensors, since it is advantageous for its availability in semiconductor electronics foundries, the technology of silicon segmentation have been developed during years and it is radiation hard. Detector designs for future accelerators (such as Future Circular Collider FCC, Electron Ion Collider EIC or the Circular Electron Positron Collider CEPC) include tracking layers with silicon detectors. Besides high-energy particle physics experiments, cancer treatment facilities such as hadron therapy centres can use large area strip detectors for beam monitoring and imaging, to provide in time information of the particles while treatment is done.

Strip detectors are well-suited to cover large area, due to their lower power consumption and fabrication cost

with respect to pixel detectors. To date, strip sensors are fabricated in production lines with a mask that covers the full area of the wafer with a photolithography resolution of ~ 800 nm. Using CMOS (Compatible Metal Oxide Semiconductor) production lines for strip sensors could open the door to more processing foundries, with the caveat that strip implants have to be stitched, using multiple reticles for a strip production. One of the challenges for passive CMOS strip sensors is proving that the stitching does not affect the performance of the strips.

For this project, two 1 cm² reticle masks were used to fabricate 2.1 cm and 4.1 cm long strip detectors. Figure 1 shows a picture of a 4.1 cm long strip sensor with the position of the stitching marked with vertical dashed lines. The reticle is repeated four times along the strip. The second reticle has the strip AC and DC pads to one side and the ending of the strip to the other side (the strip end and closing bias and guard rings).

The strips were fabricated in an LFoundry [1] 150 nm

* Corresponding author

process, stitching the two reticles with a stepper motor. The fabrication used a 150 μm thick p-type float zone wafer with a resistivity around 3 – 5 $\text{k}\Omega\text{cm}$.

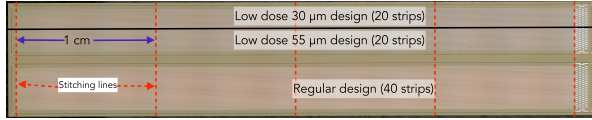


Figure 1: 4.1 cm long strip sensor. It shows the stitching lines and the two different strip designs configuration.

As shown in figure 1, each die houses two strip detectors, each one with 40 strips. There is a *regular design* (see figure 2) which is similar to the ATLAS experiment phase 2 upgrade strip design, and a *low dose design* (see figure 3) which has some features of the CMOS technology steps such as including a MIM (metal-insulator-metal) capacitor and an n-well implant. The n-well implant of the *low dose design* has two different implant widths, 20 strips have a 30 μm implant width, and 20 strips have a 55 μm n-well implant width.

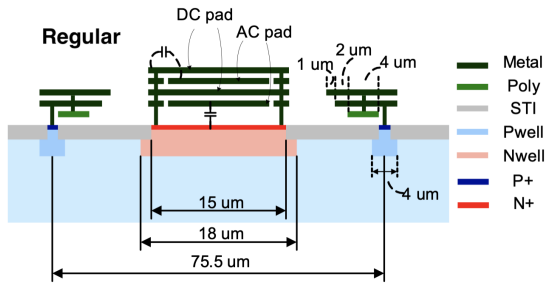


Figure 2: Regular strip design sketch.

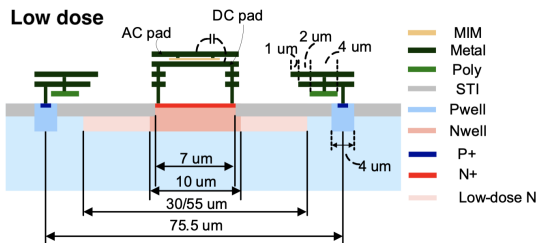


Figure 3: Low dose strip design sketch. It features two low-dose n-wells widths, 30 and 55 μm .

A first sensor batch underwent a backside processing that was not optimized and had early break down once the sensors were reaching full depletion, shown in Ref. [2]. For the next batches, the backside processing was improved and those sensors have stable current up to

300 V, they reach full depletion at ~ 35 V, with excellent results and not showing any effect of the stitching. Those sensors were irradiated with neutrons, tested in beam lines, with transient current technique and charge collection lab set-ups[3, 4, 5, 6, 7, 8]. Simulations about possible stitching scenarios show that stitching should not affect the performance of the implant of the strip [9].

Here we will show the results of passive CMOS strip detectors irradiated at CERN[10] in the IRRAD facility with 24 GeV protons at $5 \times 10^{14} \text{ n}_{\text{eq}}/\text{cm}^2$ and $1 \times 10^{15} \text{ n}_{\text{eq}}/\text{cm}^2$ fluences to study the effects of proton irradiation. The irradiation collimator is 1 cm^2 big, therefore the sensors were tilted during irradiation in order to receive the particle beam along the full area. The irradiations were carried out at room temperature.

This paper shows the electrical characterization and charge collection measurements with a ^{90}Sr radioactive source for the proton irradiated passive CMOS strip detectors, with the aim to investigate the effects of proton irradiation.

2. Electrical characterisation

Current voltage characteristics of the reverse bias were measured with a wafer prober MPI-TS3500-SE, connected to a Keithley 2410 high voltage power supply. High voltage was applied to the sensors between the bias pad and the backplane. Figure 4 shows the current voltage characteristics of the sensors for the two different fluences without annealing. Measurements were taken at -20°C and show the average of five consecutive measurements per voltage step. The detectors used for this study are the 4.1 cm long sensors.

Afterwards, the sensors were annealed for 80 min at 60°C . Figure 5 shows the current voltage characteristics after annealing. As expected, after the beneficial annealing the leakage current decreases. The break down voltage is not yet reach at 500 V.

From the leakage current the current-related damage rate (α) can be calculated with the expression[11]:

$$\Delta I_L = \alpha \phi_{\text{eq}} V$$

where ΔI_L is the difference between leakage currents at 20°C due to irradiation, ϕ_{eq} is the neutron equivalent fluence and V is the volume of the sensor. The temperature scaling from -20°C to 20°C is done with the method described in Ref. [12]. Figure 6 shows the current-related damage rate at 400 V calculated from the leakage current of figure 5 (after annealing). Low dose design shows a higher current-related damage rate than

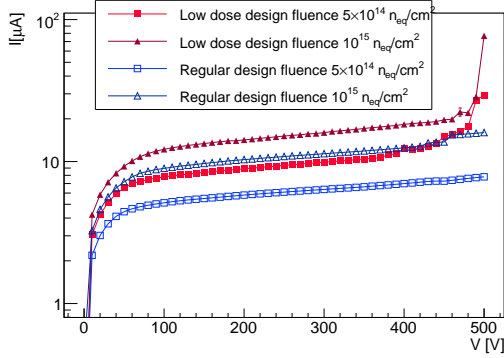


Figure 4: Current-voltage characteristics of the sensors after irradiation at $-20\text{ }^{\circ}\text{C}$.

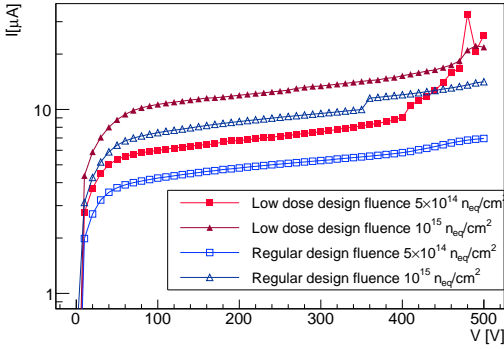


Figure 5: Current-voltage characteristics of the sensors after irradiation at $-20\text{ }^{\circ}\text{C}$, with an annealing of 80 min at $60\text{ }^{\circ}\text{C}$.

the regular design since they show higher leakage current.

Moreover, to investigate the full depletion voltage after irradiation, a capacitance voltage measurement was conducted with a HP4284A LCR-meter. The measurements were taken at a 1 kHz frequency and at $-20\text{ }^{\circ}\text{C}$. Figure 7 shows the capacitance voltage characteristics for the sensors after annealing. The capacitance reaches a plateau after $\sim 50\text{ V}$ for the fluence of $5 \times 10^{14}\text{ n}_{\text{eq}}/\text{cm}^2$, while for the $1 \times 10^{15}\text{ n}_{\text{eq}}/\text{cm}^2$ irradiated sensors, the regular design reach a plateau at $\sim 70\text{ V}$ and the low dose design at $\sim 80\text{ V}$.

From the depletion voltage, the effective doping can be estimated using the relation:

$$N_{\text{eff}} = \frac{2\epsilon_0\epsilon_{\text{Si}}V_{\text{FD}}}{q \cdot d^2}$$

Where ϵ_0 is the vacuum permittivity, ϵ_{Si} is the silicon permittivity, V_{FD} is the full depletion voltage, q is the electron charge and d is the sensor thickness. For

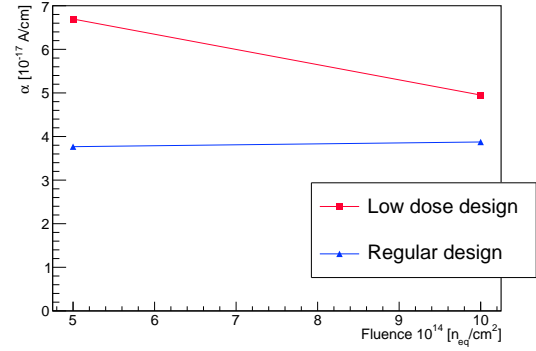


Figure 6: Current-related damage rate at 400 V of the passive CMOS strip detectors for different fluences, with an annealing of 80 min at $60\text{ }^{\circ}\text{C}$.

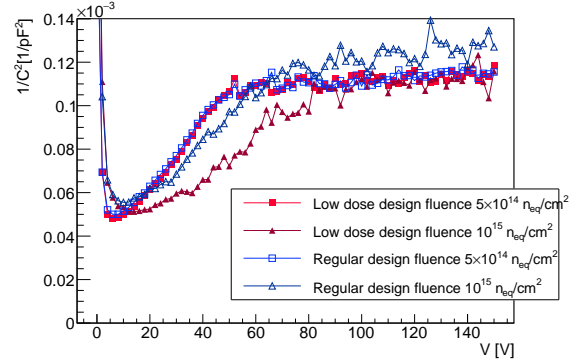


Figure 7: Capacitance voltage characteristics of the sensors after irradiation at $-20\text{ }^{\circ}\text{C}$, with an annealing of 80 min at $60\text{ }^{\circ}\text{C}$.

an unirradiated sample, the V_{FD} is 30 V for low dose design and 35 V for the regular design, that gives an effective doping of $1.7 \times 10^{12}\text{ cm}^{-3}$ and $2 \times 10^{12}\text{ cm}^{-3}$ respectively. Figure 8 shows the effective doping with the fluence. Although the bulk doping should be the same for regular and low dose designs, the effective doping shows a dependence on the strip design, inverting the behaviour of the low dose design: for unirradiated sensors low dose design show lower effective doping than the regular design, while for higher fluences the low dose design shows higher effective doping than the regular design.

3. Charge collection measurements

The two irradiated sensors were then bonded to an ALiBaVa Daughter board[13]. The daughter board is then connected to the ALiBaVa mother board which

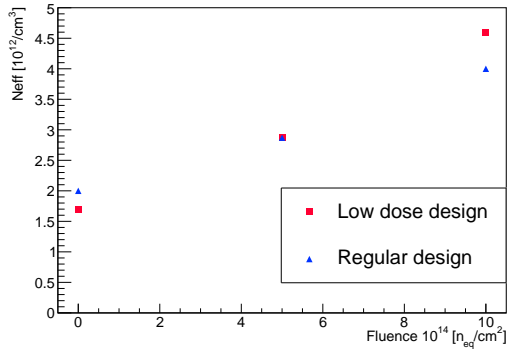


Figure 8: Effective doping of the sensors at different fluences.

reads out the bonded channels and the data is acquired with a computer. A scintillator was located under the sensor to externally trigger the signal. All the measurements were taken at -20°C . On top of the sensor, a ^{90}Sr beta source was positioned that was simultaneously exposing the sensor and the scintillator to electrons.

Figure 9 and figure 10 show the collected charge of the detector after being irradiated with $5 \times 10^{14} \text{ n}_{\text{eq}}/\text{cm}^2$ and $1 \times 10^{15} \text{ n}_{\text{eq}}/\text{cm}^2$ respectively and annealed for 80 min at 60°C . For this measurement, low dose $30 \mu\text{m}$ and low dose $55 \mu\text{m}$ are separated since individual strips can be masked. The chips were previously calibrated with another sensor, therefore the charge is shown in electrons instead of Analogue to Digital Converter units.

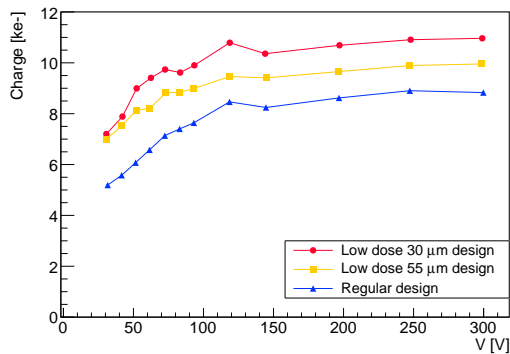


Figure 9: Collected charge measurement at -20°C from a sensor irradiated with a fluence of $5 \times 10^{14} \text{ n}_{\text{eq}}/\text{cm}^2$, after an annealing of 80 min at 60°C .

Figure 9 (sensor irradiated at $5 \times 10^{14} \text{ n}_{\text{eq}}/\text{cm}^2$ fluence) shows higher collected charge for the low dose designs, almost equal to unirradiated values ($\sim 11\,000$ electrons), while the regular design has a noticeable decrease of collected charge. On the

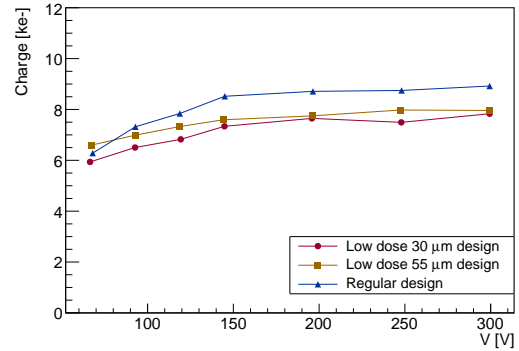


Figure 10: Collected charge measurement at -20°C from a sensor irradiated with a fluence of $1 \times 10^{15} \text{ n}_{\text{eq}}/\text{cm}^2$, after an annealing of 80 min at 60°C .

other hand, the sensors irradiated with $1 \times 10^{15} \text{ n}_{\text{eq}}/\text{cm}^2$ shown in figure 10 have the opposite behaviour. The alpha parameter decreases for the low dose design, while staying nearly constant for the regular design. This behaviour cannot be associated to the bulk damage since that should be the same for all the designs but to differences from the strip design. Besides the differences between designs, the results show very good charge collection for passive CMOS strip detectors after proton irradiation and do not show any stitching effect.

4. Summary and Conclusion

Passive CMOS strip detectors do not show any impact from stitching in their performance as shown here and in previous results. The irradiation with protons shows some differences between the two designs used, low dose and regular, decreasing the performance of low dose design for higher fluences.

The successful performance of the passive CMOS strip detectors and the fact that the stitching does not show any effect for particle detection opens the door for the CMOS foundries to fabricate strip sensors. Future experiments may use stitched strip sensors since it is not affecting the efficiency. Besides that, future strip productions are investigating to include active parts, with electronics embedded in the silicon, therefore producing the first Monolithic Active Strip Sensors (MASS) and avoid future hybridisation steps for strips.

5. Acknowledgements

The authors acknowledge the usage of the wafer prober at the TU Dortmund. Funded by the

Deutsche Forschungsgemeinschaft (DFG, German Research Foundation)- 450639102.

References

- [1] LFoundry s.r.l. Landshut, Ludwig-Erhard-Strasse 6a, 84034 Landshut, Germany, 2024.
- [2] L. Diehl et al., *Characterization of passive CMOS strip sensors*, Nuclear Instruments and Methods in Physics Research A **1033** (2022) 166671.
- [3] L. Diehl et al. Evaluation of passive CMOS strip sensors, Nuclear Instruments and Methods in Physics Research A, 1039 (2022) 167031.
- [4] M. Baselga et al., Passive CMOS Strip Detectors Response with Alpha Particles, Proceedings of Science, VERTEX2023, 067.
- [5] I. Zatocilova et al., Characterisation, simulation and test beam data analysis of stitched passive CMOS strip sensors, NIMA 1061 (2024) 169132.
- [6] N. Davis et al., Characterisation and simulation of stitched CMOS strip sensors, NIMA 1064 (2024) 169407.
- [7] I. Zatocilova et al., Passive CMOS Strip Sensors – Characterisation, Simulation and Test Beam Results, PoS(ICHEP2024)1073.
- [8] N. Davis et al., TCAD simulation of stitching for passive CMOS strip detectors, Volume 1080, November 2025, 170807.
- [9] M. Baselga et al., TCAD simulation of stitching for passive CMOS strip detectors, 2025 JINST 20 C01027.
- [10] PS-IRRAD Proton Facility, CERN, Switzerland
- [11] G Lindstrom, Radiation damage in silicon detectors, Nuclear Instruments and Methods in Physics Research A 512 (2003) 30–43.
- [12] A. Chilingarov, Temperature dependence of the current generated in Si bulk, 2013 JINST 8 P10003
- [13] R. Marco-Hernández et al., *A portable readout system for silicon microstrip sensors*, Nuclear Instruments and Methods in Physics Research A 623 (2010) 207-209.